Journal of Pharmaceutical Innovation (2019) 14:141–151
https://doi.org/10.1007/s12247-018-9342-0

ORIGINAL ARTICLE

A New Modeling Approach of Ultrasonic Extraction of Polyphenols from Carob

Karim Kriaa [1,2] · Bilel Hadrich [3]

Abstract

Purpose A new approach was proposed to model the extraction kinetics according to the operating parameters. This approach is based on the determination of the critical time t_c (a characteristic time which depends on the operating parameters).

Methods It is necessary to start by collecting the experimental values of t_c from experimental kinetics using the second derivation of extraction yield. Then, a full factorial design 2^3 is used to model t_c as function of studied factors: temperature, solid-liquid ratio and ultrasonic power. The obtained expression of t_c was used in second time as the basis of the modeling of extraction kinetics. It made possible to locate the inflection point that separates the two intervals of the extraction. To assure continuity in this point, we changed variable of time for the second phase of extraction and we started fitting from the last calculated point from the first phase. Seven models were tested to fit studied kinetics.

Results A mathematical model was proposed to express t_c according to the operating parameters of the studied extraction. Patricelli (composed of two exponential terms) and the exponential models showed the best fitting results for all experiments. Patricelli model fitted very well the first phase of experiments and the exponential model fitted the second phase.

Conclusion This confirms a new coupled washing/diffusion hypothesis of extraction performing in three steps: washing, first diffusion step, and second diffusion step.

Keywords Ultrasound · Extraction kinetic modeling · Full factorial design · Carob (*Ceratonia silique* L.) · Polyphenols

Introduction

Extraction is frequently used in our daily life from preparing tea to doing laundry. The principle of extraction is very simple, and it consists of passing compounds from one phase to another. However, there is much subtlety because separations go against a thermodynamic intuition, and entropy is obtained by dispersion and not by separation. Many phenomena can take place and interpretation is difficult.

Several studies continue to deepen on the extraction and mainly with the use of new technologies such as ultrasounds, microwaves, and supercritical fluids. Different vegetable sources were studied such as grape pomace [1], grape marc [2], black chokeberry [3], lemongrass (*Cymbopogon flexuosus*) [4], microalga (*Chlorella* sp.) [5] and carob [6–8]. Generally, the studies consist of the description of the kinetics or see the effect of the operating parameters on the extraction yield to optimize the processes.

In our study, we propose a new approach to explain a remarkable behavior that is often neglected by the researchers and considered as an experimental error. In fact, we suppose that the extraction kinetics can be influenced by the non-uniformity of the vegetable matrix which is generally constituted of a number of layers with different densities and compositions.

Problematic

Extraction kinetics has always been a tendency to an equilibrium stage. It starts with a maximum rate and stabilizes to zero

✉ Bilel Hadrich
bilel.hadrich@enis.tn

[1] Department of Chemical Engineering, National School of Engineers of Gabes, University of Gabes, Gabes, Tunisia

[2] College of Engineering, Al Imam Mohammad Ibn Saud Islamic University (IMSIU), PO Box 5701, Riyadh 11432, Saudi Arabia

[3] Unité de Biotechnologie des Algues, Biological Engineering Department, National School of Engineers of Sfax, University of Sfax, Sfax, Tunisia

(the equilibrium). A typical extraction kinetics (Fig. 1) presents a first fast step of washing dominated by solute partition then a slow step of diffusion controlled by solute diffusion [10–13].

Several mathematical models can verify this progress, and generally laws of power can describe the asymptotic behavior.

During our studies on extraction, we noticed an evolution of kinetics on two stages as shown in Fig. 2.

A bibliographic study required to understand this aspect. The same behavior was found but we notice that authors neglect this variation in kinetics and they consider it as errors due to manipulation. This occurrence has been observed in several extraction studies of bioactive components (such as polyphenols, active ingredients …) from different vegetal matrices by using various extraction techniques (ordinary extraction, ultrasound, high-pressure CO_2, pulsed electric fields, high-voltage electrical discharges …). Figure 3 shows six examples (from literature) of extraction kinetics [1, 3, 14–17].

The usual mathematical models do not describe this look. This is a two-stage kinetics. Two stages are noted, and three steps will be assumed: washing step (I), a first diffusion step (II), and a second diffusion step (III).

The first stage contained step (I) and step (II); then, the second stage contained step (III) is characterized by the appearance of a second bearing corresponding to a second diffusion equilibrium. The time of appearance of the second diffusion depends on the operating conditions. This critical time noted t_c and will be modeled according to the operating parameters.

For this, we must find t_c (beginning of the second stage). After that, we can study the effect of operating parameters on its variation. Then, we propose a mathematical model of the extraction kinetics.

Material and Methods

Sample Preparation

Dried carob pods from the local market of Sfax—south of Tunisia—were packet stored at room temperature ($T = 20 \pm 2$ °C) in burlap sacks. Samples were deseeded and cut just into two halves before the extraction process. The size of the carob samples was $2.0 \pm 0.2 \times 1 \pm 0.1$ cm^2 and their moisture content was $17 \pm 2.6\%$ d.b.

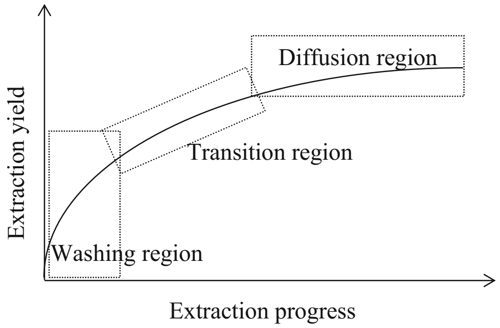

Fig. 1 Typical extraction kinetics with three regions: a washing region, a diffusion region, and a transitional region, adapted from [9]

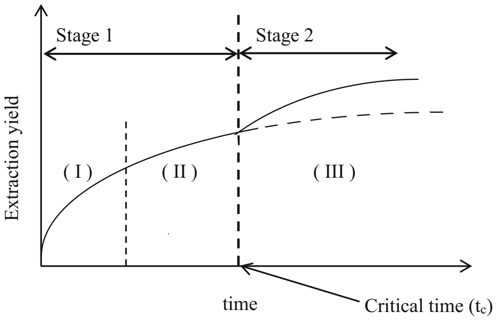

Fig. 2 Observed curve of extraction yield versus time

Experimental Setup and Methods of Extraction

The used experimental system is 1-L agitated reactor equipped with an ultrasonic generator [3, 8]. Agitation was fixed at 400 min^{-1}. A temperature control system was used to keep the medium temperature constant. Sample preparation and polyphenol concentration were determined by using the same method presented by Hadrich et al. [8]. The extraction yield (%) is calculated by Eq. 1:

$$Y = \frac{Content\ of\ polyphenols}{Maximum\ content\ of\ polyphenols} \times 100 \tag{1}$$

Determination of Critical Time (t_c)

The first step is to identify critical time (t_{ci}) for each experiment i ($1 \le i \le 8$). For thus, the first derivation $(dY/\mathrm{d}t)_i$ and the second derivation $(d^2Y/\mathrm{d}t^2)_i$ of extraction yield were calculated. The two derivations were obtained by a polynomial regression (within a sliding interval) using "polyfit" and "polyder" Matlab functions. In fact, the "polyfit" function is used to fit the best second order polynomial equation for each three successive experimental points (by iterative calculation) and "polyder" function calculates the corresponding derivation.

The time t_{ci} is defined as the beginning of the second increasing stage of extraction yield after stabilization (end of step (II)–beginning of step (III), Fig. 2).

At the end of step (II) (Y almost constant): $(dY/\mathrm{d}t)_i \rightarrow 0$.

At the beginning of the step (III), $(dY/\mathrm{d}t)_i$ follows a sharp increase. This is expressed mathematically by a maximum value of $(d^2Y/\mathrm{d}t^2)_\mathrm{i}$. Thus, the t_{ci} value finally corresponds to the maximum value of $(d^2Y/\mathrm{d}t^2)_i$.

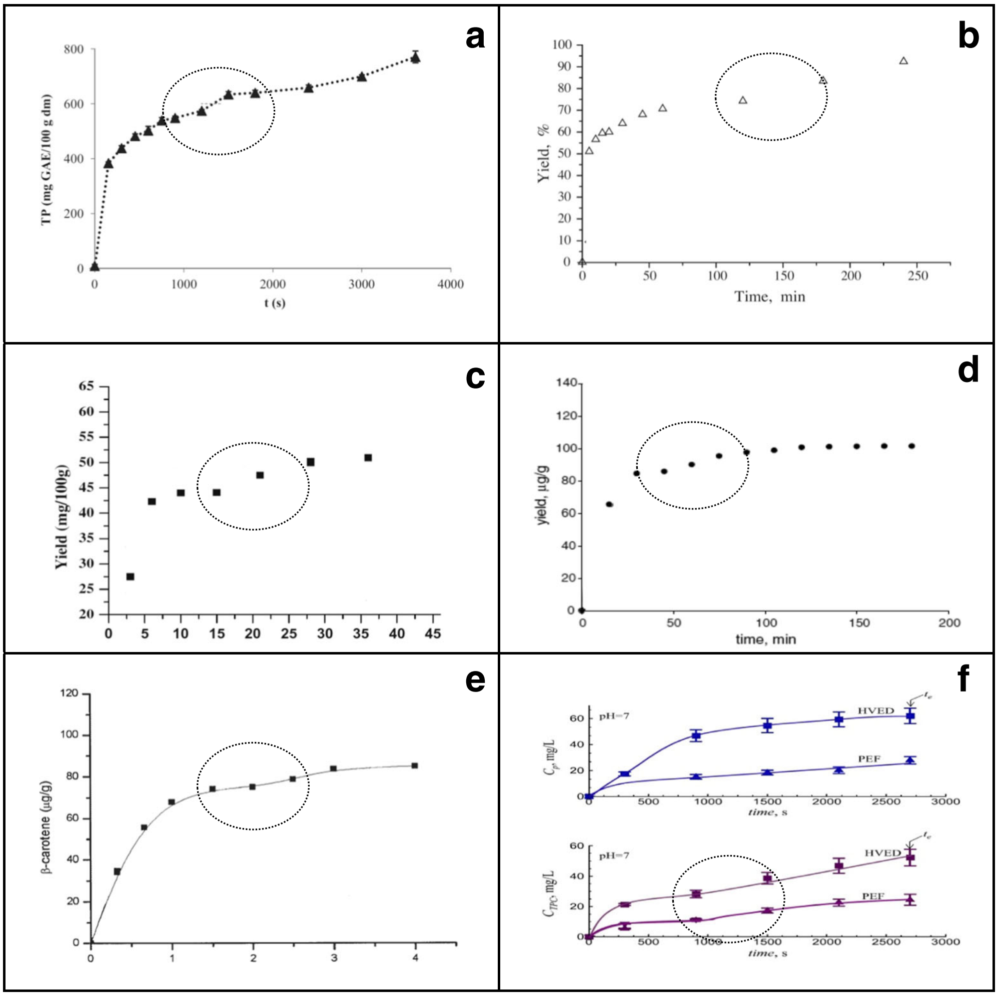

	Extract	Sources	Techniques	Reference
a	Polyphenols	grape pomace	Ultrasound	[1]
b	Polyphenols	black chokeberry	Ultrasound	[3]
c	Anthocyanins	red cabbage	High pressure CO_2	[14]
d	Active ingredients	medicinal plants	In water - ethanol	[15]
e	β-carotene	*Rosa canina*	In petroleum ether	[16]
f	Proteins Polyphenols	papaya peels	Pulsed electric fields and high voltage electrical discharges	[17]

Fig. 3 Examples of kinetics extraction from bibliography

Modeling of Critical Time (t_c) Using an Experimental Design

A 2^3 experimental design was used to study the effect of three factors and their interactions, on the critical time value (t_c). Table 1 shows maximum (+1) and minimum (−1) levels for each factor. In fact, ultrasonic was operated in continuous mode with and without power (100 W and 0 W, respectively) at fixed frequency of 30.8 kHz. Chosen levels for temperature and solid-liquid ratio (noted by S) were 40–60 °C and 1:3–1:19 *w*/*v*, respectively.

The experimental response t_c was modeled using the following equation:

$$t_c = \beta_0 + \sum_{j=1}^{m} \beta_j \cdot X_j + \sum_{j=1}^{m-1} \sum_{k>j}^{m} \beta_{jk} \cdot X_j \cdot X_k + \varepsilon \qquad (2)$$

where β_0 is the constant term, $\beta_j$and β_{jk} are the regression coefficients, ε is the error between calculated and experimental data, X_j are the factors and m is the number of factors.

A reduced regression model shown only the significant variables, was determined after testing coefficients by the analysis of variance test (ANOVA) at 95% significance level

Table 1 Full factorial design 2^3 and experimental response

Experiment	T (Temperature in °C)	S (Solid-liquid ratio in *w*/*v*)	P (Utrasonic power in W)	Critical time (t_c in min)
1	− 1 (40)	− 1 (1:3)	− 1 (0)	90.24
2	+ 1 (60)	− 1 (1:3)	− 1 (0)	91.49
3	− 1 (40)	+ 1 (1:19)	− 1 (0)	114.07
4	+ 1 (60)	+ 1 (1:19)	− 1 (0)	122.59
5	− 1 (40)	− 1 (1:3)	+ 1 (100)	39.28
6	+ 1 (60)	− 1 (1:3)	+ 1 (100)	50.66
7	− 1 (40)	+ 1 (1:19)	+ 1 (100)	52.89
8	+ 1 (60)	+ 1 (1:19)	+ 1 (100)	76.49

corresponding to a probability value $p < 0.05$. The design and all analysis of the full factorial design were performed with Minitab (Minitab Inc.) Release 16.0 statistical package.

Mathematical Models

Seven mathematical models were chosen from literature to predict the yield as function of extraction time: [18]; Eq. 3); Power model ([19]; Eq. 4); Parabolic diffusion model ([20, 21]; Eq. 5); Elovich model ([22]; Eq. 6); Exponential model (Eq. 7); Weibull model (Eq. 8); and Patricelli model ([23]; Eq. 9). All models were applied to all experimental kinetics.

Peleg Model

$$Y(t) = \frac{t}{\frac{1}{K_1} + \frac{1}{K_2} \times t} \tag{3}$$

where K_1 is Peleg's rate constant (min g/mg) and K_2 is Peleg's capacity constant (g/mg) ($K_2 \leq 1$).

Power Model

$$Y(t) = K_1 \times t^{K_2} \tag{4}$$

where K_1 is a constant incorporating the characteristics of the carrier-active agent system (min^{-K_2}) and K_2 is diffusion exponent. For the extraction from vegetal material, $K_2 < 1$.

Parabolic Diffusion Model

$$Y(t) = K_1 + K_2 \cdot t^{\frac{1}{2}} \tag{5}$$

where K_1 is washing coefficient and K_2 is diffusion rate constant ($\text{min}^{-0.5}$).

Elovich Model

$$Y(t) = \frac{1}{K_1} \cdot \ln(K_1 \cdot K_2) + \frac{1}{K_1} \cdot \ln(t) \tag{6}$$

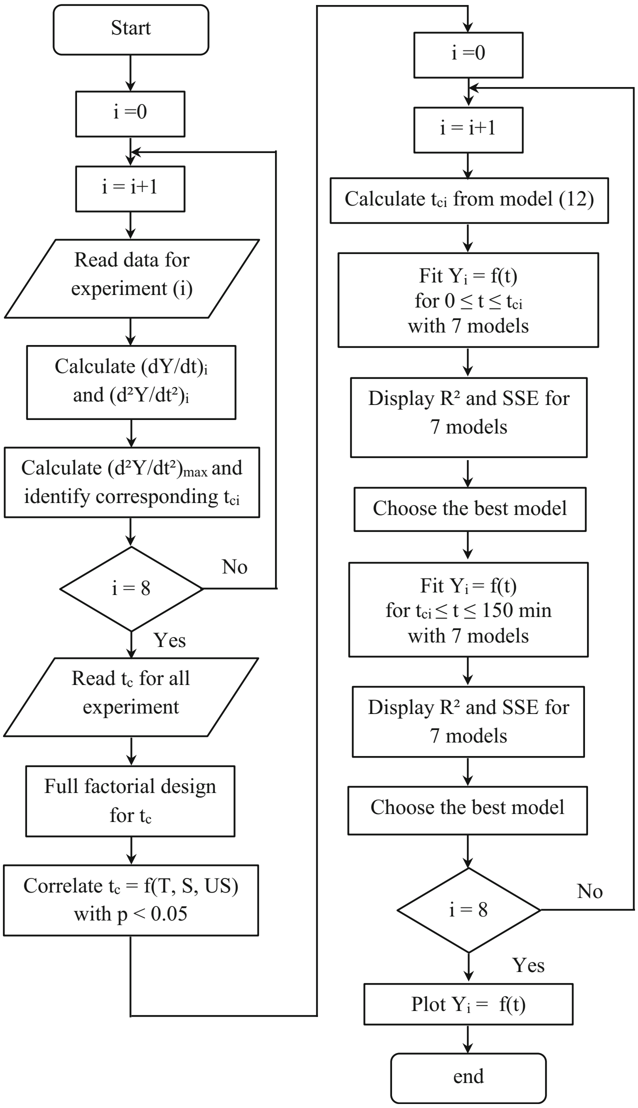

Fig. 4 Organigram of numerical treatment

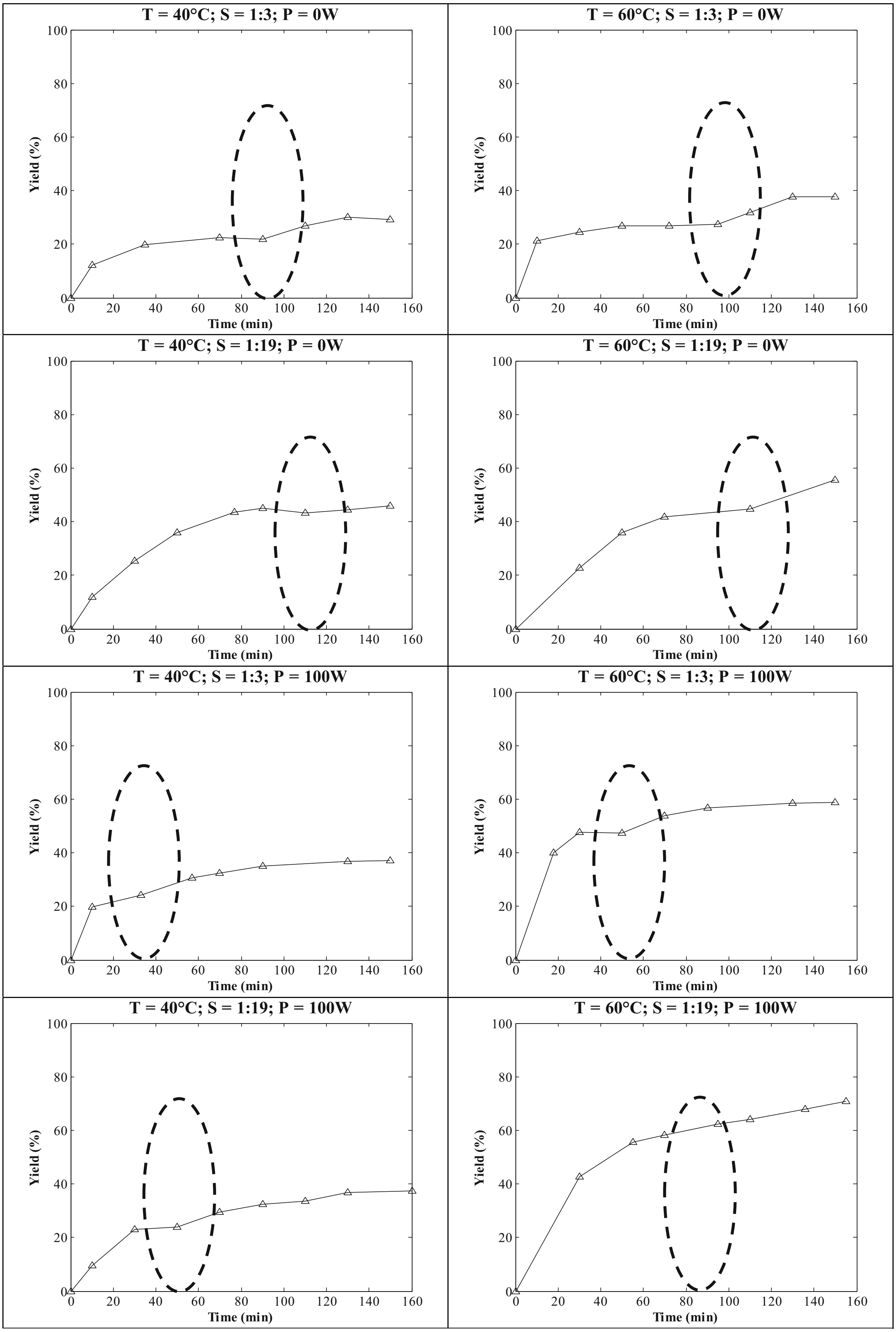
T = 40°C; S = 1:3; P = 0W

T = 60°C; S = 1:3; P = 0W

T = 40°C; S = 1:19; P = 0W

T = 60°C; S = 1:19; P = 0W

T = 40°C; S = 1:3; P = 100W

T = 60°C; S = 1:3; P = 100W

T = 40°C; S = 1:19; P = 100W

T = 60°C; S = 1:19; P = 100W

Fig. 5 Experimental yield (Δ) versus extraction time for all studied conditions; in dotted the starting area of the second stage

Fig. 6 Photography of cutted carob pod

where K_1 is a coefficient of Elovich's equation (g biomass d.b./mg GAE) and K_2 is a coefficient of Elovich's equation (mg GAE/g biomass d.b. min).

Exponential Model

$$Y(t) = A\cdot(1 - \exp(-K_1\cdot t)) \tag{7}$$

where A is the highest yield and K_1 is a constant (min^{-1}).

Weibull Model

$$Y(t) = 1 - \exp\left(-\left(\frac{t}{K_1}\right)^{K_2}\right) \tag{8}$$

where K_1 is a scale parameter, which is related to the reciprocal of the extraction rate constant and K_2 is a shape parameter. In the case of extraction $K_2 < 1$.

Patricelli Model

$$Y(t) = A\cdot(1 - \exp(-K_1\cdot t)) + B\cdot(1 - \exp(-K_2\cdot t)) \tag{9}$$

where A and B are final yield (hypothetical) in solution due to the washing step and the diffusion step, respectively, and K_1 and K_2 are kinetic coefficient for the washing step and the diffusion step, respectively.

Statistical Tests of Fitting Quality

Studied models were checked to fit experimental kinetics with its two phases using nonlinear least squares regression method carried out with Matlab, R2010a (The MathWorks, Inc.). Coefficient of determination (R^2) and sums of squared error (SSE) show the fitting quality of models. The corresponding equations are presented:

$$R^2 = 1 - \frac{\sum_{i=1}^{n}\left(Y_i - \hat{Y}_i\right)^2}{\sum_{i=1}^{n}\left(Y_i - \overline{Y}\right)^2} \tag{10}$$

$$SSE = \sum_{i=1}^{n}\left(Y_i - \hat{Y}_i\right)^2 \tag{11}$$

with Y_i: experimental yield; $\hat{Y}_i$: calculated yield by using regression model; $\overline{Y}$: arithmetic average of experimental yield; n: number of experimental points.

All models' coefficients were calculated with 95% confidence limits (i.e., $p < 0.05$).

Data Treatment Organigram

At first, a Matlab program was developed to find the critical time t_c for all experiments. Then, a full factorial experimental design 2^3 will be proposed to model t_c as function of operating parameters: temperature, solid-liquid ratio, and ultrasound power. After that, a second Matlab program was developed, to test the fitting quality of seven studied models, for kinetics extraction involving the two suggested extraction stages delimited by the time t_c. This program is applied for all extraction conditions to find all mathematic parameters, for the best model fitting the extraction kinetics with two phases.

The second Matlab program used for fitting the extraction kinetics follow the organigram shown in Fig. 4.

After inputting experimental points of kinetics extraction (presented as yield versus time, $Y_i = f(t)$; $1 \leq i \leq 8$ experiments):

- The time t_{ci} will be determined for all conditions and a full factorial experimental design 2^3 will be used to model $\tilde{t}_{ci} = f(T, S, P)$; with T: temperature; S: solid-liquid ratio; P: ultrasonic power. The influencing factors are defined with an ANOVA test for $p < 0.05$.
- Fitting step is based on the separation of the kinetics extraction in two stages; the first one containing steps (I) and (II) of Fig. 2 and the second stage containing the latest step (III). Then, the fitting will be performed on

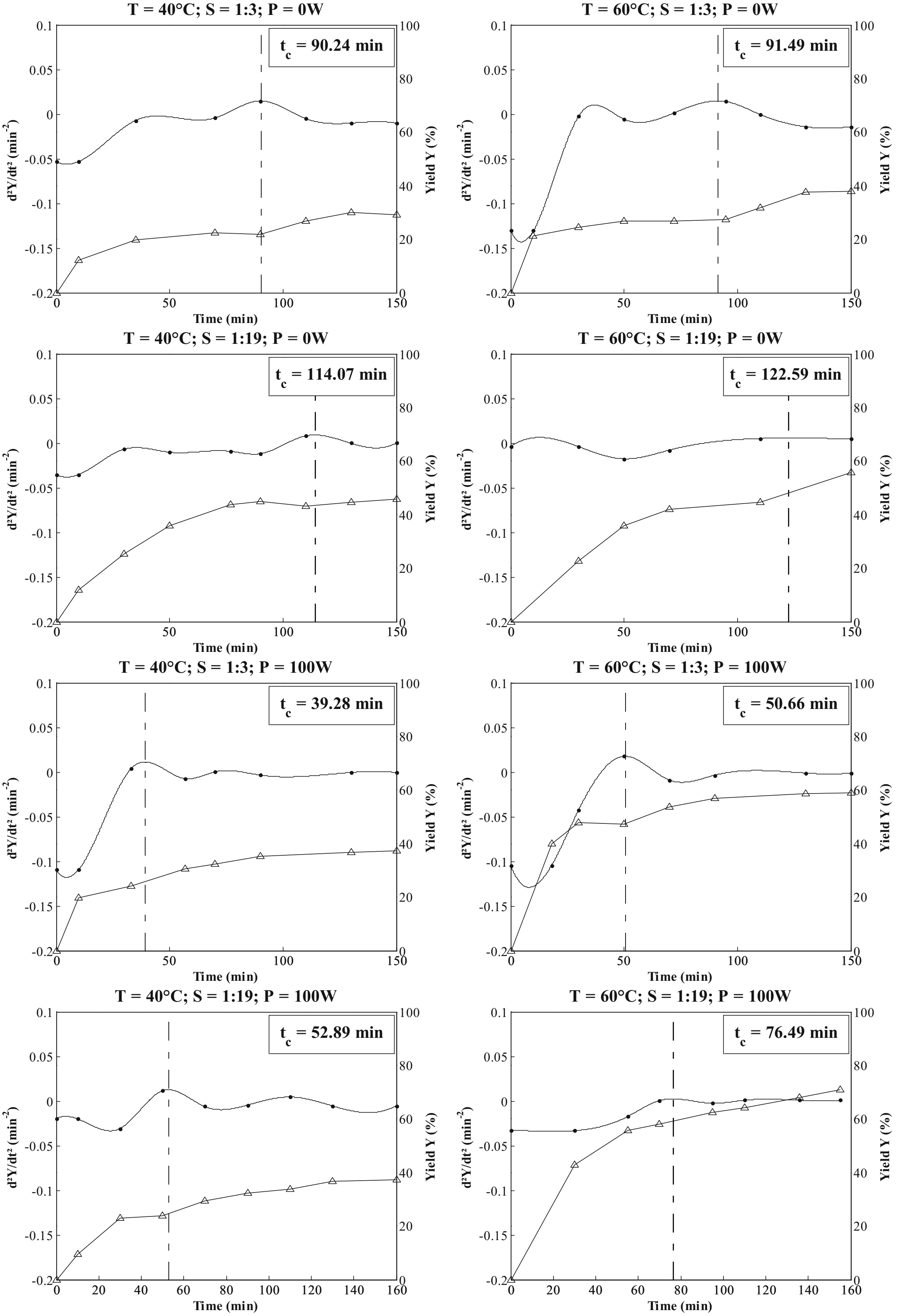

Fig. 7 Variation of d^2Y/dt^2 (●) and Y (Δ) versus extraction time for all studied experimental conditions. Dashed lines: experimental t_c

Table 2 Analysis of variance for the factors and the interactions model of the responses

Source	Degree of freedom	Sum of square (SS)	Adjusted sum of square (adj SS)	Adjusted mean square (adj MS)	*F* value	*p* value
Main effects	3	6317.14	6317.14	2105.71	687.51	0.028*
T	1	250.32	250.32	250.32	81.73	0.070^{NS}
S	1	1113.21	1113.21	1113.21	363.46	0.033*
P	1	4953.61	4953.61	4953.61	1617.34	0.016*
2-way interactions	3	156.92	156.92	52.31	17.08	0.176^{NS}
T × S	1	47.48	47.48	47.48	15.50	0.158^{NS}
T × P	1	79.44	79.44	79.44	25.94	0.123^{NS}
S × P	1	29.99	29.99	29.99	9.79	0.197^{NS}
Residual error	1	3.06	3.06	3.06		
Total	7	6477.12				

S = 1.75009, PRESS = 196.02. R^2 = 99.95%, R^2 (pred) = 96.97%, R^2 (adj) = 99.67%

All variables are in coded units, *T* is the coded value of temperature (°C), *S* is the coded value of; solid-liquid ratio (*w*/*v*), *P* is the coded value of ultrasonic power (W)

NS not significant

*Significant at the level 5%

two intervals [0, t_{ci}] and [t_{ci}, 150], for each experiment. The value of t_{ci}, used in this part, is calculated using the established model described above (Eq. 2).

Results and Discussion

Experimental Results

Figure 5 shows eight kinetics of extraction at different conditions of temperature, solid-liquid ratio, and ultrasonic power. It is noted that the extraction kinetics presents a rise at two stages. However, the second stage's appearance time varies with operational parameters from 30 min to 2 h of extraction. This phenomenon may be explained by the presence of two layers presenting different textures as shown in Fig. 6. Those behave as two consecutive sources of polyphenols. Therefore, two successive extractions are from two solid matrices of different structures: a first layer, easily releasing his exracts, that is enveloped in a another harder and more compact protective skin which releases its extracts after some delay of swelling. The more the operating parameters favor the puffing, the more the appearance time of the second stages will be reduced. As described in Fig. 2, stage 1 and stage 2 contain a washing phase (I) and a two diffusion steps (II and III). And, the second extraction operates after a characteristic delay called critical time t_c which characterizes the swelling time, and which is directly related to the operating parameters.

Determination of the Critical Time t_c

The determination of the critical time t_c is important to delimit the two stages of the extraction kinetics and it is indispensable for the modeling study of t_c according to the operating conditions.

The time t_c corresponds to a second rise in the kinetics of extraction after a first stabilization (first stage) which mathematically corresponds to a maximum second derivative of the yield (d^2Y/dt^2).

The Matlab software was used to determine the critical time t_c and we started by collecting the experimental data by the function "xlsread"; then, we calculate the maximum of the second derivative using the function "max"; then, we plot in dashed lines with dots ($x = t_c$).

Figure 7 shows the result of the experimental time t_c with the kinetics yield as a function of extraction time.

Full Factorial Experimental Design for Critical Time t_c

The critical time, t_c, was determined and presented in experiment matrix (Table 1). The response t_c was found in range from 39.28 to 122.59 min (less than 160 min). The value of t_c depends on the tested experimental conditions. Therefore, the ANOVA test is applicable in this case. In fact, the presence of a multi-linear dependence of t_c on the different tested factors and their interactions required this statistical test to determine the significant effects from all of them. Table 2 presents the result of ANOVA test. Only main effects, solid-liquid ratio (*S*) and ultrasonic power (*P*), are significant ($p < 0.05$).

The largest effect decreasing the t_c value is the power of ultrasound with a *p* value of 0.016 (versus 0.033 for solid-liquid ratio). All interactions are insignificant. High coefficient of determination ($R^2 = 99.95\%$) and high adjusted coefficient of determination ($R^2(\text{adj}) = 99.67\%$) indicate the validity of the multi-linear model for t_c response. The very low standard error of the multi-linear regression ($S = 1.750$) proves

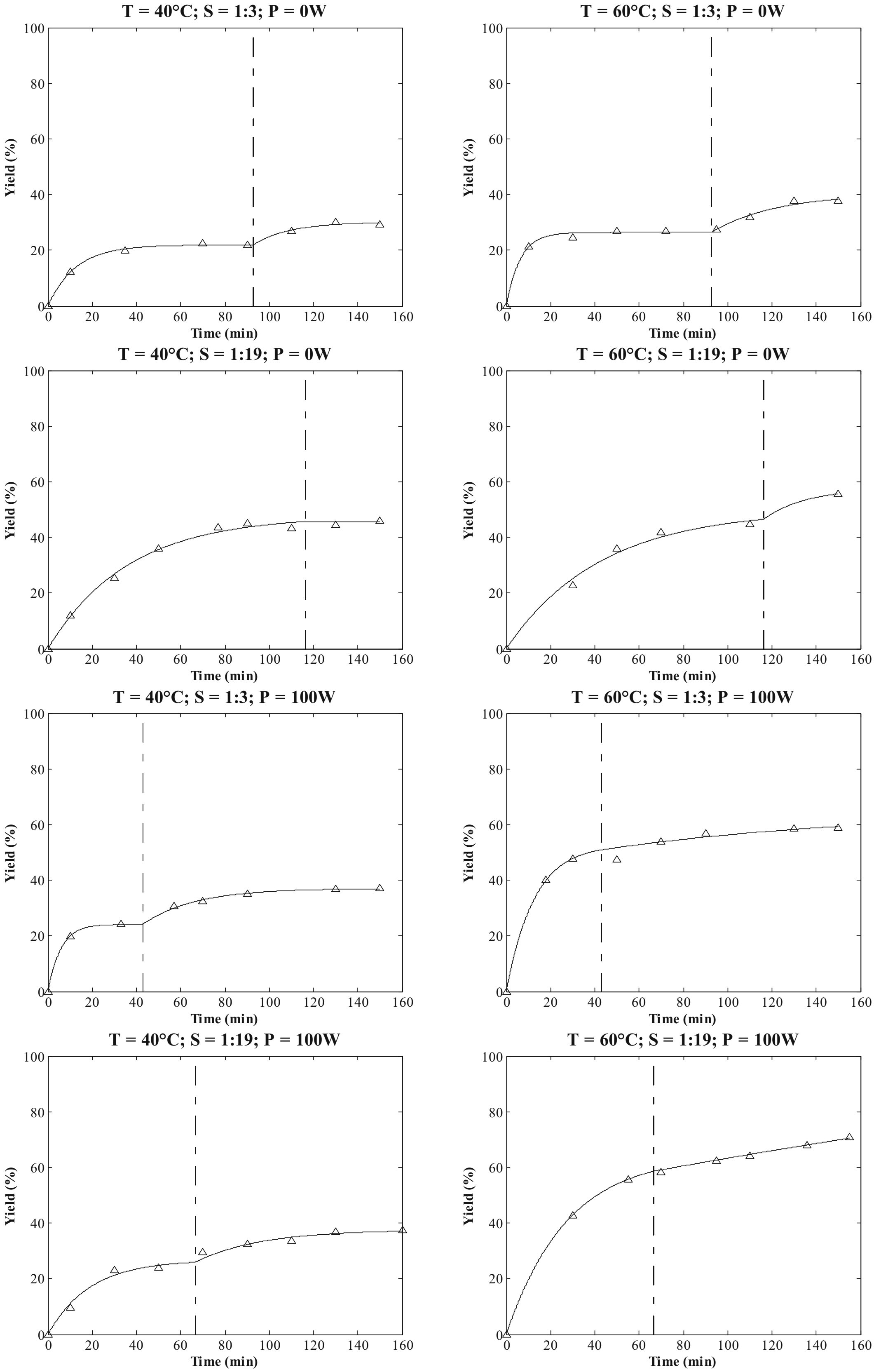

Fig. 8 Modeling results of all experimental extraction conditions. Δ: experimental data; continuous lines: model; dashed lines: calculated t_c

Table 3 Modeling results of experimental data ($p < 0.05$)

	Step 1: $A \times (1 - \exp(-K_1 \times t)) + B \times (1 - \exp(-K_2 \times t))$						Step 2: $A' \times (1 - \exp(-K'_1 \times t))$			
	Statistics		Patricelli et al. model parameters				Statistics		Exponential model parameters	
	R^2	SSE	A	K_1	B	K_2	R^2	SSE	K''_1	A'
Exp. 1	0.998	6.036×10^{-5}	0.163	0.055	0.060	0.206	0.796	1.144×10^{-4}	6.241×10^{-2}	0.081
Exp. 2	0.999	3.767×10^{-5}	0.096	0.041	0.179	0.637	0.899	2.378×10^{-4}	3.380×10^{-2}	0.140
Exp. 3	0.994	1.202×10^{-3}	0.092	0.028	0.384	0.027	0.807	1.491×10^{-4}	1.429×10^{-3}	2.963×10^{-3}
Exp. 4	0.990	1.334×10^{-3}	0.497	0.023	0.001	0.809	1.000	7.812×10^{-18}	5.183×10^{-2}	0.111
Exp. 5	1.000	7.105×10^{-4}	0.002	0.017	0.242	0.172	0.972	8.917×10^{-5}	4.232×10^{-2}	0.129
Exp. 6	1.000	5.255×10^{-4}	0.002	0.733	0.527	0.078	0.761	2.197×10^{-3}	8.383×10^{-3}	0.142
Exp. 7	0.986	5.606×10^{-4}	4.831×10^{-4}	0.034	0.264	0.054	0.844	6.599×10^{-4}	3.388×10^{-2}	0.116
Exp. 8	1.000	5.493×10^{-4}	3.701×10^{-4}	0.727	0.642	0.037	0.985	1.490×10^{-4}	1.470×10^{-3}	0.972

this hypothesis. Therefore, maintained model is expressed by Eq. 12:

$$\tilde{t}_c = 79.71 + 11.80 \cdot S - 24.88 \cdot P \qquad (12)$$

This agrees with our hypotheses. Thus, the ultrasound power is the most influential parameter in the reducing of time t_c (this explains the minus sign of $-24.88 \cdot P$). Ultrasounds allow exploiting the hard layer of our plant source and extract the contained polyphenols. However, the solid-liquid ratio has a latecomer effect by increasing the time t_c (the positive sign of $+11.80 \cdot S$) because it reduces the specific ultrasonic energy per unit mass.

Equation 12 will be the basis of our modeling study. It will be possible to define the two intervals of time corresponding to the two extraction stages. These two stages will be successively modeled by testing seven mathematical models for each extraction.

Modeling Results

In this study, modeling starts by the determination of the two extraction stages for experiment i ($1 \leq i \leq 8$). For this, t_{ci} values were calculated from Eq. 12 for each experiment. Figure 8 shows the calculated t_{ci} for each experiment, corresponds already to the end of stage 1 of the extraction kinetics ($Y = f(t)$). This result approves very well the fundamental hypothesis of the present work.

After that, the seven presented models in the "Mathematical models" section were tested to fit the first extraction stage (for $0 \leq t \leq t_{ci}$). Statistical parameters (R^2 and SSE) are the criteria for choosing the best model. The same seven models' equations were tested similarly for the second phase (for $t_{ci} \leq t \leq t_{final}$). In order to have continuity in fitting results, we change the variable according to Eq. 13:

$$Y = f(\tau) + Y_c \qquad (13)$$

with

$\tau = t\text{-}t_{ci}$;

Y_c: yield at the time t_{ci} calculated with the best model for the first step (%).

The same statistical criteria for choosing the best model are retained (R^2 and SSE).

Both Patricelli and exponential models were retained for the first and the second stages, respectively, showing the best regression results for all experiments (Table 3). It can be observed that the fitting quality is characterized by a high R^2 (between 0.761 and 1) and an insignificant SSE (between 7.812×10^{-18} and 2.197×10^{-3}), in both stages. All models' parameters are also determined, with a high significance level (95%), for the two identified extraction kinetics stages (Table 3). Those results show the importance of the fitting protocol established in this work using the presented fundamental hypothesis.

A good agreement between experimental and modeling data can be observed during all extraction time (for the two stages), for all established experiments (Fig. 8). It can be noted that the models chosen by the performed program check 56 experimental points from 57. Generally, we have not seen such result in bibliography (particularly at the end of kinetics extraction) and the gap between experiment and modeling results was explained as operational errors even if experiment was made at triplicate.

Conclusions

Ultrasound extraction of the polyphenols from carob kibbles was studied. In this work, extraction kinetics show two increasing stages. This behavior has been observed in several works in literature on extraction of bioactive extracts from various vegetal matrices. This phenomenon can be explained by two consecutive sources of extracts from non-uniform solid matrix. Therefore, two stages of extraction and through three steps were noted: washing, first diffusion, and second diffusion. Then, the second extraction stage was considered operating after a critical delay t_c. A new approach based on a mathematical investigation is proposed to model the observed extraction kinetics.

Firstly, a mathematical protocol was carried out to determinate the critical time t_c which separate the different extraction stages.

Secondly, a full factorial experimental design was used to express t_c as function of operating parameters. Only ultrasonic power and solid-liquid ratio are significant and the largest effect decreasing the t_c value is the power of ultrasound (P), for 95% significance level.

Then, the experimental data are fitted on both stages. Patricelli model and exponential model were chosen from seven tested models, to fit the first and the second extraction stages, respectively. They show the best fitting result for all tested conditions (high R^2 and insignificant SSE).

This work was carried out on the ultrasonic extraction of polyphenols from carob. However, it can be generalized to other vegetable sources to describe the kinetics of other extracts and to examine the effects of other extraction techniques (such as microwaves and supercritical extraction), on the reducing of the critical time t_c to accelerate the apparition of the second stage, corresponding to the maximum of the extraction yield.

References

1. González-Centeno MR, Comas-Serra F, Femenia A, Rosselló C, Simal S. Effect of power ultrasound application on aqueous extraction of phenolic compounds and antioxidant capacity from grape pomace (*Vitis vinifera* L.): experimental kinetics and modelling. Ultrason Sonochem. 2015;22:506–14.
2. Tao Y, Zhang Z, Sun DW. Kinetic modeling of ultrasound-assisted extraction of phenolic compounds from grape marc: influence of acoustic energy density and temperature. Ultrason Sonochem. 2014;21:1461–9.
3. Galvan d'Alessandro L, Kriaa K, Nikov I, Dimitrov K. Ultrasound assisted extraction of polyphenols from black chokeberry. Sep Purif Technol. 2012;93:42–7.
4. Balti MA, Hadrich B, Kriaa K, Kechaou N. Lab-scale extraction of essential oils from Tunisian lemongrass (*Cymbopogon flexuosus*). Chem Eng and Process. 2018;124:164–73.
5. Hadrich B, Akremi I, Dammak M, Barkallah M, Fendri I, Abdelkafi S. Optimization of lipids' ultrasonic extraction and production from *Chlorella* sp. using response-surface methodology. Lipids Health Dis. 2018;17:87.
6. Almanasrah M, Roseiro LB, Bogel-Lukasik R, Carvalheiro F, Brazinha C, Crespo J, et al. Selective recovery of phenolic compounds and carbohydrates from carob kibbles using water-based extraction. Ind Crop Prod. 2015;70:443–50.
7. Cháfer A, Berna A. Study of kinetics of the D-pinitol extraction from carob pods using supercritical CO_2. J Supercrit Fluids. 2014;94:212–5.
8. Hadrich B, Dimitrov K, Kriaa K. Modelling investigation and parameters study of polyphenols extraction from carob (*Ceratonia silique* L.) using experimental factorial design. J. Food Process. Preserv. 2017;41(2):e12769. https://doi.org/10.1111/jfpp.12769 .
9. Raynie DE. Extraction. In: Wilson ID, editor. Encyclopedia of separation science. Oxford: Academic Press; 2000. p. 118–28.
10. Chan C-H, Yusoff R, Ngoh G-C. Modeling and kinetics study of conventional and assisted batch solvent extraction. Chem Eng Res Des. 2014;92:1169–86.
11. Franco D, Sineiro J, Pinelo M, Núñez MJ. Ethanolic extraction of *Rosa rubiginosa* soluble substances: oil solubility equilibria and kinetic studies. J Food Eng. 2007;79:150–7.
12. Perez EE, Carelli AA, Crapiste GH. Temperature-dependent diffusion coefficient of oil from different sunflower seeds during extraction with hexane. J Food Eng. 2011;105:180–5.
13. So GC, Macdonald DG. Kinetic of oil extraction from canola (rapeseed). Can J Chem Eng. 1986;64:80–6.
14. Xu Z, Wu J, Zhang Y, Hu X, Liao X, Wang Z. Extraction of anthocyanins from red cabbage using high pressure CO_2. Bioresour Technol. 2010;101:7151–7.
15. Taralkar SV, Garkal DJ. Solid-liquid extraction process of active ingredients from medicinal plants mathematical modes. Int J Chem Sci Appl. 2010;1(2):82–5.
16. Sturzoiu A, Stroescu M, Guzun AS, Dobre T. Empirical models applied for kinetics extraction of β-carotene from *Rosa canina*. Rev Chim. 2011;62(3):344–8.
17. Parniakov O, Barba FJ, Grimi N, Lebovka N, Vorobiev E. Impact of pulsed electric fields and high voltage electrical discharges on extraction of high-added value compounds from papaya peels. Food Res Int. 2014;65:337–43.
18. Peleg M. An empirical model for the description of moisture sorption curves. J Food Sci. 1988;53:1216–9.
19. Sinclair GW, Peppas NA. Analysis of non-Fickian transport in polymers using simplified exponential expressions. J Membrane Sci. 1984;17:329–31.
20. Kim JY, Kim CL, Chung CH. Modeling of nuclide release from low-level radioactive paraffin waste: a comparison of simulated and real waste. J Hazard Mater. 2002;94(2):161–78.
21. Kitanović S, Milenović D, Veljković VB. Empirical kinetic models for the resinoid extraction from aerial parts of St. John's wort (*Hypericum perforatum* L.). Biochem Eng J. 2008;41:1–11.
22. Low MJD. Kinetics of chemisorption of gases on solids. Chem Rev. 1960;60(3):267–312.
23. Patricelli A, Assogna A, Casalaina A, Emmi E, Sodini G. Fattori che influenzano l'estrazoine dei lipidi da semi decorticate di girasole. Riv Ital Sostanze Gr. 1979;56:136–42.